Sol–gel-generated La_2NiO_4 for CH_4/CO_2 reforming

B.S. Liu [a,b] and C.T. Au [b,*]

[a] Department of Chemistry, Tianjin University, Tianjin 300072, P.R. China
[b] Department of Chemistry and Centre for Surface Analysis and Research, Hong Kong Baptist University, Kowloon Tong, Hong Kong, China

Received 2 July 2002; accepted 28 October 2002

A stable La_2NiO_4 catalyst active in CH_4/CO_2 reforming has been prepared by a sol–gel method. The catalyst was characterized by techniques such as XRD, BET, TPR and TG/DTG. The results show that the conversions of CH_4 and CO_2 in CH_4/CO_2 reforming over this catalyst are significantly higher than those over a Ni/La_2O_3 catalyst prepared by wet impregnation and those over a La_2NiO_4/γ-Al_2O_3 catalyst. The TG/DTG outcome confirmed that the amount of carbon deposition observed in the former case was less than that observed in the latter two cases, a phenomenon attributable to the uniform dispersion of nanoscale Ni particles in the sol–gel-generated La_2NiO_4 catalyst.

KEY WORDS: CH_4/CO_2 reforming; sol–gel-generated La_2NiO_4.

1. Introduction

The CO_2 reforming of methane is industrially attractive because it yields syngas with a H_2/CO ratio suitable for Fischer–Tropsch synthesis [1]. The conversion of CH_4 and CO_2 into value-added chemicals can ameliorate the emission of greenhouse gases; and the process is environmentally friendly [2–5]. From a commercial viewpoint, a nickel catalyst is more economical than a catalyst of precious metal; hence, the engineering of a stable and active nickel catalyst for CH_4/CO_2 reforming has been the goal of many researchers [6–8]. Recently, extensive studies have been conducted on CH_4/CO_2 reforming over supported Ni-based catalysts such as Ni–alkaline earth oxides [9], Ni/La_2O_3 [6,10,11], Ni/Al_2O_3 [12–15], Ni–CaO [9,10,16], Ni–MgO [9,17] and Ni/MgO–CaO [18]. In general, carbon deposition on a nickel catalyst during CO_2 reforming of methane is rapid [17]. Recently, we have generated a La_2NiO_4 catalyst by means of a sol–gel method from a metal complex precursor and observed satisfactory performance of the catalyst in CH_4/CO_2 reforming.

2. Experimental

2.1. Catalyst preparation

Stoichiometric $Ni(NO_3)_2{\cdot}6H_2O$ and La_2O_3 (molar ratio of Ni and La was 1:2) were dissolved completely in diluted nitric acid, and citric acid and ethylene glycol were added to the solution. The molar amounts of citric acid and ethylene glycol were 1.5 times that of the total metal ions. Then, the solution was heated to 60 °C with constant stirring. After the removal of water through evaporation, a translucent green gel was formed. Next, the cogel obtained was aged and dried in a beaker at room temperature (RT) for 3 days; subsequently, it was calcined at 500 °C for 3 h and at 800 °C for 5 h. This sol–gel-generated catalyst will be referred to as "La_2NiO_4 (sol–gel)" hereafter. For comparison, a Ni/La_2O_3 catalyst (by incipient wetness impregnation [6]) and a 9% La_2NiO_4/γ-Al_2O_3 (i.e. Ni was 9 wt% of the catalyst) catalyst were also prepared. For the synthesis of the latter, aluminum isopropoxide (20 g) was hydrolyzed with 150 ml of deionized water at 80 °C, and the mixture was kept at 80 °C for 1.5 h with vigorous stirring. Then, 0.01 mol of nitric acid was added for peptization and the sol was refluxed at 95 °C for 1 h with stirring to obtain a clear sol. Then 6.49 g of $Ni(NO_3)_2{\cdot}6H_2O$ and 5.8 g of La_2O_3 were dissolved in 15 ml of 20% HNO_3. This solution was added to the clear boehmite sol and the mixture was refluxed at 95 °C for 16 h with vigorous stirring. The obtained cogel was put in a beaker for solvent evaporation at RT. Finally, the dry cogel was calcined at 800 °C for 4 h.

2.2. Characterization of catalyst

The adsorption–desorption isotherm of N_2 and pore size distribution of the catalysts were measured using N_2 as an adsorbate with a NOVA-1200 instrument at 77 K. X-ray diffraction (XRD) experiments were carried out using a Rigaku automatic diffractometer (Rigaku D-MAX) with monochromatized CuKα radiation ($\lambda = 0.15406$ nm) at a setting of 40 kV and 70 mA. The patterns recorded were referred to the powder diffraction files 1998 ICCD PDF Database for identification.

* To whom correspondence should be addressed.
E-mail: pctau@hkbu.edu.hk

1011-372X/03/0200-0165/0

Temperature-programmed reduction (TPR) was carried out according to the following procedure. The sample was heated from RT to 300 °C at a rate of 10 °C/min in a flow of N_2 (45 ml/min), and was kept at this temperature for 30 min. The sample was then cooled to RT and the carrier gas was switched to a 5% H_2/N_2 mixture (flow rate of 45 ml/min). A linear rise in temperature from RT to 950 °C at a rate of 10 °C/min was adopted. The amount of hydrogen consumption was measured by means of a thermal conductivity detector (TCD).

Temperature-programmed desorption (TPD) of O_2 was carried out in a quartz microreactor connected to a mass spectrometer (HP GCD-1800A). After a sample was pretreated and swept with helium to obtain a stable baseline, the desorption sequence was started at a helium flow of 30 ml/min and a heating rate of 10 °C/min. The effluent was monitored by means of a GC–MS system (GCD, HP G1800A).

TGA experiments were conducted using a Shimadzu DT-40 thermal analyzer. Typically, the sample (~10 mg) was heated from 40 to 900 °C at a rate of 20 °C/min in air with a flow rate of 50 ml/min.

2.3. Catalytic activity

The CO_2 reforming of methane was carried out at 700 °C over a fixed-bed quartz reactor (i.d. 10 mm) at a gas hour space velocity (GHSV) of 4.8×10^4 ml/g/h. The catalyst was secured inside the reactor with the void space below packed with quartz sand and quartz wool. The temperature was measured with a K-type thermocouple located inside the reactor but without direct contact with the catalyst. Before the CH_4/CO_2 reaction, the catalyst was reduced in a flow of H_2 (40 ml/min) at 700 °C for 1 h. The gas effluent was analyzed by means of on-line gas chromatography (Shimadzu 8A, TCD). A Porapak Q and a 5 A sieve column were used for gas separation. The conversion of CO_2 or CH_4 was defined as converted CO_2 or CH_4 per total amount of CO_2 or CH_4. The selectivity of CO (calculated based on total carbon conversion) and H_2 (assuming that a molar CH_4 is converted into 2 mol of H_2), as well as the yield of carbon (including the carbon of heavier hydrocarbons condensable in the transfer line) are defined as follows:

$$S_{CO}(\%) = 100 \times [CO]_o/(([CO_2]_i - [CO_2]_o) + ([CH_4]_i - [CH_4]_o))$$

$$S_{H_2}(\%) = 100 \times [H_2]_o/(2 \times ([CH_4]_i - [CH_4]_o))$$

$$Y_C(\%) = 100 \times (([CO_2]_i + [CH_4]_i) - ([CH_4]_o + [CO_2]_o + [CO]_o))/([CO_2]_i + [CH_4]_i)$$

where $[CO_2]_i$ and $[CH_4]_i$ are inlet flow rates, and $[CH_4]_o$, $[CO_2]_o$, and $[CO]_o$ are outlet flow rates.

3. Results and discussion

3.1. Characterization of catalysts

According to the results of BET studies, La_2NiO_4 (sol–gel) is a mesoporous material with a specific surface area (9.3 m^2/g) significantly larger than that (4.2 m^2/g) of Ni/La_2O_3. With γ-Al_2O_3 being the support material, the specific surface area of the La_2NiO_4/γ-Al_2O_3 catalyst was about 38.3 m^2/g. Figure 1 shows the pore size distribution and pore volume of La_2NiO_4 (sol–gel) and La_2NiO_4/γ-Al_2O_3. The pore diameter of the former was about 3.0 nm and remained unchanged after 80 h of CH_4/CO_2 reforming; as for the latter, the pore diameter was 7.5 nm. In addition, compared to the case of La_2NiO_4/γ-Al_2O_3, the pore volume of La_2NiO_4 (sol–gel) was small; the apparent increase after the CH_4/CO_2 reforming reaction was due to the carbon nanotubes formed during the reaction.

The TPR profiles of La_2NiO_4 (sol–gel), NiO and La_2NiO_4/γ-Al_2O_3 are shown in figure 2. In the case of La_2NiO_4 (sol–gel), beside the big peaks at ~400 and 620 °C, there is a shoulder peak at 580 °C. Comparing with the TPR spectrum of NiO, the peak at about 400 °C is assigned to the reduction of NiO. The peak at around 620 °C and the shoulder at 580 °C could be related to the reduction of surface and bulk La_2NiO_4 (sol–gel), respectively. For La_2NiO_4/γ-Al_2O_3, a large peak at about 400 °C, two small ones at around 350 and 550 °C, and a large broad one at 780 °C were observed. In previous TPR studies on the reducibility of nickel aluminate, a temperature above 800 °C was required for the reduction of stoichiometric $NiAl_2O_4$ [19] and a peak at about 750 °C was interpreted as the reduction of non-stoichiometric nickel aluminate in Ni/γ-Al_2O_3 [20]. We considered that the broad peak at around 800 °C corresponded to the reduction of $NiAl_2O_4$; it indicates that in the presence of γ-Al_2O_3, there is La_2NiO_4 decomposition and $NiAl_2O_4$ formation (figure 2).

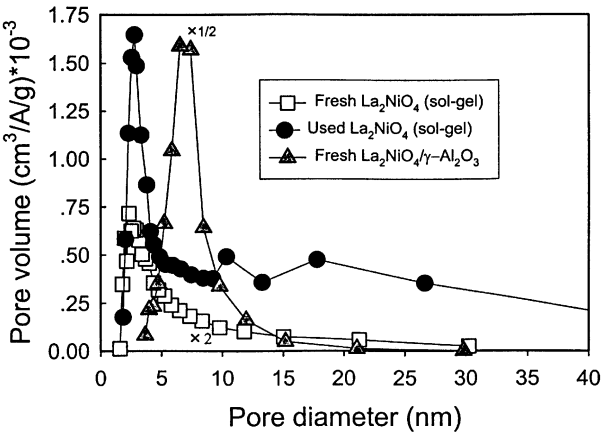

Figure 1. Pore size distribution of fresh and used La_2NiO_4 (sol–gel), and fresh 9% La_2NiO_4/γ-Al_2O_3.

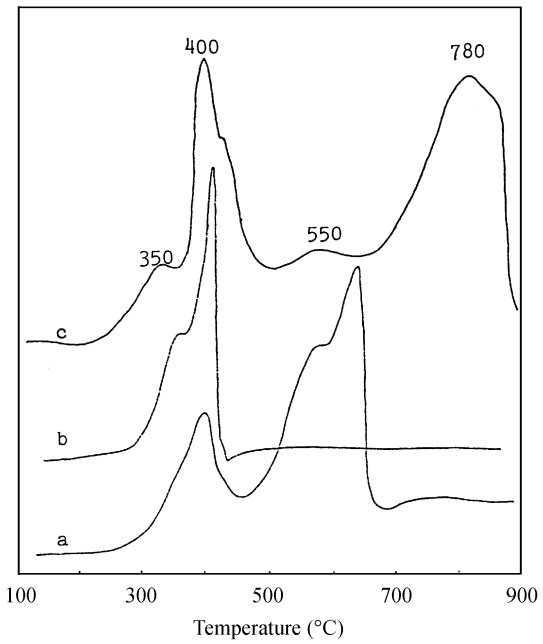

Figure 2. TPR profiles of (a) La_2NiO_4 (sol–gel) (10.3 mg), (b) NiO (12.3 mg) and (c) 9% La_2NiO_4/γ-Al_2O_3 (40.4 mg); the data in parentheses are the mass of the samples adopted for the studies.

The results of O_2 TPD studies of fresh and O_2-treated La_2NiO_4 (sol–gel) are shown in figure 3. We found that, besides the O_2 desorption above 800 °C, a symmetric peak of O_2 desorption at ~350 °C was observed over the fresh sample (figure 3(a)), whereas an asymmetric one at ~225 °C with a tail was observed over the O_2-treated one (figure 3(b)). We suggest that the non-stoichiometric oxygen in fresh La_2NiO_4 (sol–gel) was originated from oxygen adsorption during the sample calcinations. According to Pena and Fierrio [21], a high-temperature peak (>800 °C) can be attributed to structural lattice oxygen, and a low-temperature peak to oxygen originated in the reduction process involving the Ni site cations and the formation of anion vacancies. The results indicate that non-stoichiometric oxygen in

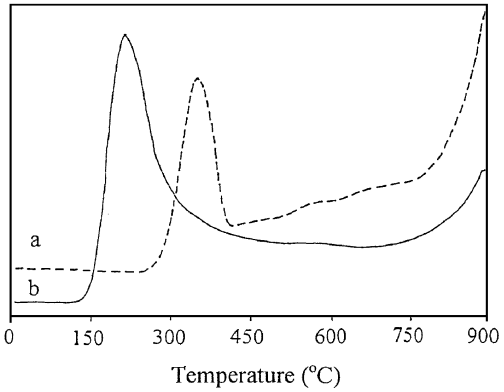

Figure 3. O_2 TPD spectra of La_2NiO_4 (sol–gel): (a) oxygen desorption of a fresh sample (after calcination in air at 800 °C); (b) the same sample was then cooled to RT and treated in O_2 (20 ml/min) at the same temperature for 1 h before TPD procedure.

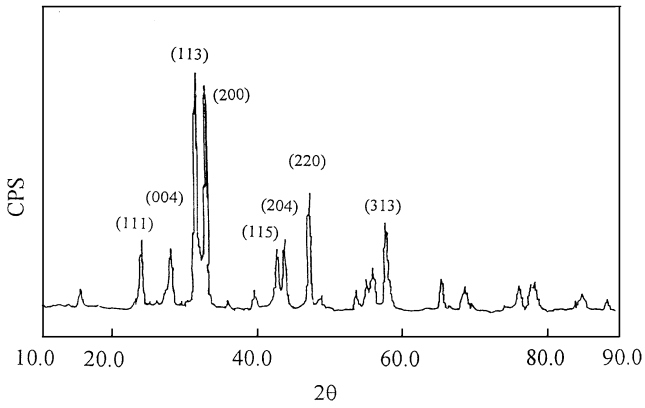

Figure 4. XRD spectrum of the La_2NiO_4 (sol–gel) catalyst.

La_2NiO_4 could be removed and replenished under various conditions as suggested before by Ren *et al.* [22]. The XRD pattern of La_2NiO_4 (sol–gel) is shown in figure 4. The results suggest a unique K_2NiF_4 (spinel) tetragonal structure of excellent crystallinity, indicating that it is possible to prepare La_2NiO_4 of spinel structure by mixing La^{3+} and Ni^{2+} in molecular level by the sol–gel technique [23]. Such a structure is favorable for stabilizing the nickel ions in the catalyst.

The results of thermal analysis of Ni/La_2O_3 and La_2NiO_4 (sol–gel) samples are shown in figure 5. The major peaks in the differential TG curves are located between RT and 600 °C. For the Ni/La_2O_3 catalyst obtained by incipient wetness impregnation of $Ni(NO_3)_2{\cdot}6H_2O$ and La_2O_3, three DTG features (figure 5(a)) were observed at 124, 359 and 460 °C, respectively. We consider the peak at 124 °C to be due to a combined loss of physisorbed water and crystallization water, and the peak at 359 °C to the decomposition of nitrate species on the support, an observation similar to the results of Ho and Chou [24]. After comparing with the decomposition of pure $Ni(NO_3)_2{\cdot}6H_2O$, we assign the DTG peaks at around 460 °C to the decomposition of $LaONO_3$ produced in the interaction of NO_3^- with La_2O_3. As for the La_2NiO_4 (sol–gel) catalyst, the DTG profile shows losses at 140, 254, 343, 412 and 500 °C. The weight losses at 140 and 254 °C can be associated with the removal of crystallization water of $Ni(NO_3)_2{\cdot}6H_2O$ and $La(NO_3)_3{\cdot}H_2O$, respectively. The small peaks at 343 °C and the large one at 412 °C are assigned to the decomposition of $Ni(NO_3)_2$ and $La(NO_3)_3$ species, respectively. The existence of two exothermal peaks in the DTA profile (figure 5(c)) of La_2NiO_4 (sol–gel) suggests that there were new compounds being formed at ~400, 485 and 500 °C, such as $LaONO_3$ and La_2NiO_4. The $LaONO_3$ decomposed at higher temperature into La_2O_3, and the weight loss at ~500 °C in figure 5(b) should be attributed to the decomposition of $LaONO_3$. The La_2O_3 generated combines evenly with NiO to form a stable spinel structure (La_2NiO_4) at ~500 °C, giving the exothermal peak at ~500 °C in figure 5(c).

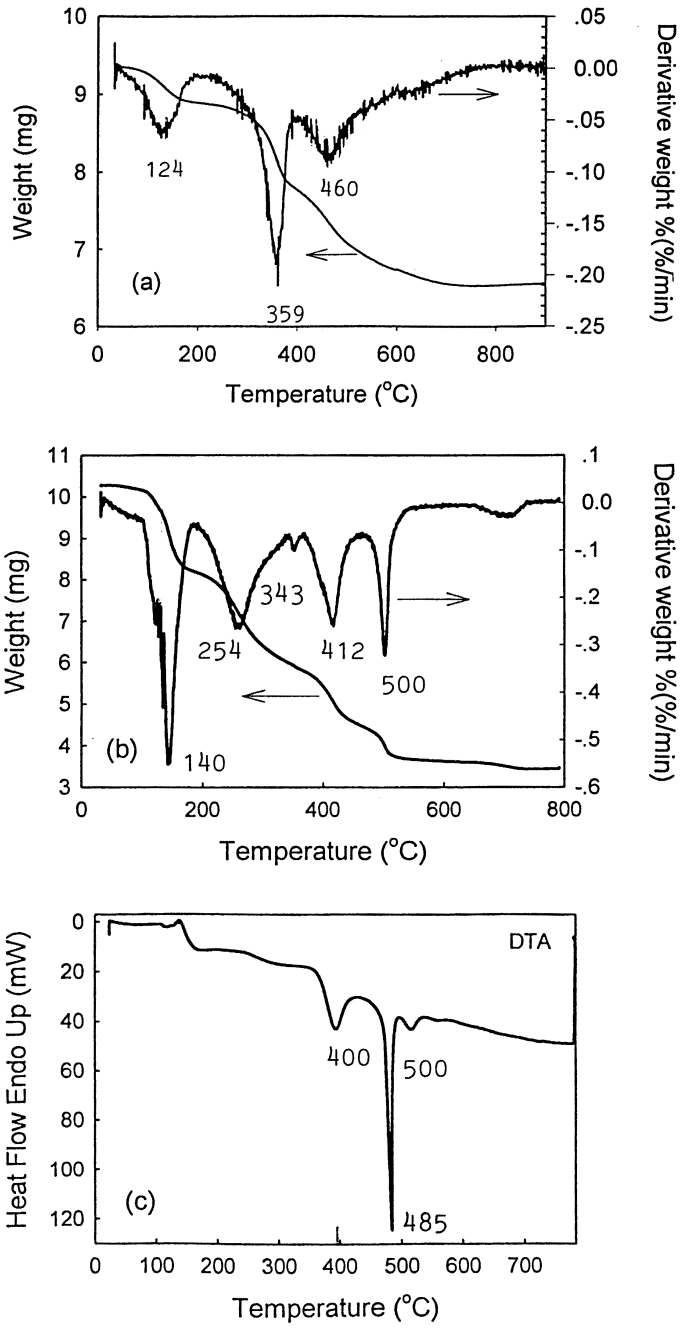

Figure 5. TG/DTG profiles of (a) Ni/La_2O_3 (impreg.) and (b) La_2NiO_4 (sol–gel); (c) DTA profile of La_2NiO_4 (sol–gel).

3.2. *Catalytic properties*

The conversions of CH_4 and CO_2 over the catalysts in CH_4/CO_2 reforming are shown in figure 6. The conversion of CH_4 over Ni/La_2O_3 was higher than those over La_2NiO_4 (sol–gel) or La_2NiO_4/γ-Al_2O_3 at the initial stage of reaction (figure 6(A)). We observed that the catalyst bed of Ni/La_2O_3 was completely blocked with a large amount of deposited carbon after 3–5 h and it becomes meaningless to take further readings. This is because CH_4 dehydrogenated rapidly on the active nickel sites and the coke was not removed efficiently by CO_2. As for the La_2NiO_4 (sol–gel) and 9% La_2NiO_4/γ-Al_2O_3 catalysts, they were still active after a reaction time of 30 h. Over La_2NiO_4 (sol–gel), CH_4 conversion was above 50% at an on-stream time of 80 h. The CH_4 conversion over La_2NiO_4 (sol–gel) was higher than that over 9% La_2NiO_4/γ-Al_2O_3 because the introduction of a γ-Al_2O_3 support favors the chemisorption as well as the disproportionation of CO [11]. According to the results of the XRD study (figure 4), the La_2NiO_4 (sol–gel) catalyst exhibited a typical spinel structure. During H_2 pretreatment at 700 °C, the Ni^{2+} ions in La_2NiO_4 were reduced to nanoscale Ni^0 particles that dispersed

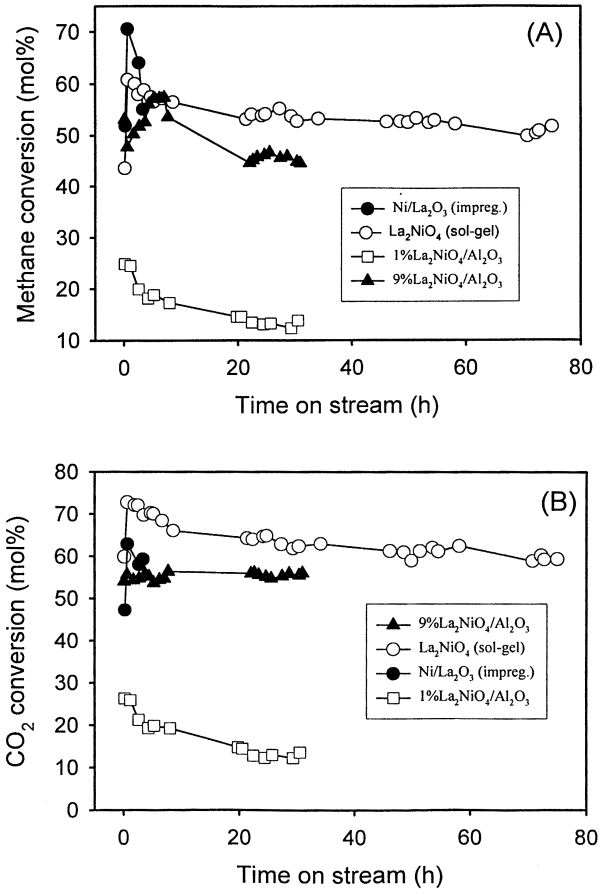

Figure 6. Conversion of (A) CH_4 and (B) CO_2 observed over Ni/La_2O_3, La_2NiO_4 (sol–gel), 9% La_2NiO_4/γ-Al_2O_3 and 1% La_2NiO_4/γ-Al_2O_3 catalysts during CO_2/CH_4 reforming at 700 °C as a function of on-stream time. GHSV = 4.8×10^4 ml/g/h, $CO_2 : CH_4 = 1 : 1$.

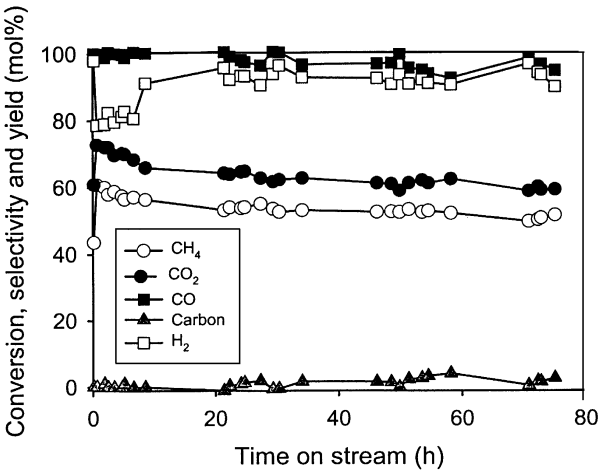

Figure 7. Conversions of CO_2 (●) and CH_4 (○), selectivities of CO (■) and H_2 (□), and yield of carbon (▲) observed over La_2NiO_4 (sol–gel) during CO_2/CH_4 reforming at 700 °C as a function of on-stream time. GHSV = 4.8×10^4 ml/g/h, $CO_2 : CH_4 = 1 : 1$.

uniformly on the surface of La_2O_3 crystallites, and remained unsintered and non-aggregated during CH_4/CO_2 reforming. On the contrary, for the Ni/La_2O_3 catalyst prepared by incipient wetness impregnation, Ni^0 particles aggregated and sintered on La_2O_3, resulting in catalytic deactivation. The CO_2 conversion observed over La_2NiO_4 (sol–gel) was higher than that observed over Ni/La_2O_3 (figure 6(B)) because the specific surface area (9.4 m^2/g) of the former is higher than that (4.2 m^2/g) of the latter. We suggested that the La_2O_3 in La_2NiO_4 (sol–gel) prevents transition metals from agglomeration and promotes the dispersion of nanoscale Ni^0 particles, resulting in an enhancement in catalytic activity and stability. In addition, we found that the conversions of CH_4 and CO_2 observed over 1% La_2NiO_4/γ-Al_2O_3 catalyst were very low; this can be due to the fact that at low nickel concentration, the number of active sites is low as well.

Figure 7 illustrates the CH_4 and CO_2 conversions, CO and H_2 selectivities and carbon yield over La_2NiO_4 (sol–gel) as a function of on-stream time. Within a period of 80 h, CO and H_2 selectivities remained at ~99 and 93%, respectively, whereas carbon yield was approximately 1–2%, significantly lower than that observed over Ni/La_2O_3 or NiO-La_2O_3/γ-Al_2O_3, indicating that the La_2NiO_4 (sol–gel) catalyst is stable and catalytically highly active. Zhang *et al.* [10] investigated CH_4/CO_2 reforming over a Ni/La_2O_3 catalyst at very low reactant conversion; the catalyst was stable within a period of 100 h, but obvious deactivations were observed when the catalyst was employed under normal reaction conditions [11]. This is in agreement with our experimental results: our Ni/La_2O_3 catalyst prepared by wet impregnation deactivated quickly and the catalyst bed was blocked in 3–5 h due to carbon deposition and/or the formation of carbon nanotubes [25].

3.3. TG/DTG investigation of carbon deposition

The DTG curves of the used catalyst (figure 8(A)) show a weight loss due to the removal of carbon. We reported previously that the weight losses at or above 650 °C are associated with the removal of filamentous carbon or graphitic carbon [26] deposited on the Al_2O_3 supports. For the Ni/La_2O_3 catalyst, a sharp weight loss at 616 °C reflects a kind of carbon deposition on the nickel active sites, most likely to be capsulated carbon; the extent of weight loss in the case of Ni/La_2O_3 was larger (figure 8(B, c)) than that of the La_2NiO_4 (sol–gel) catalyst (figure 8(B, a)). For 9% La_2NiO_4/γ-Al_2O_3 sample, there were two kinds of coke (figure 8(A, b)) on the surface. In the case of La_2NiO_4 (sol–gel), the temperature for weight losses was the highest amongst the three cases, indicating that an amorphous carbon (such as capsulated carbon) on the working catalyst transferred into inert carbon or graphitic carbon with on-stream time, a case similar to that observed over Ga–Mo/HZSM-5 catalyst [27]. Figure 8(B) shows the relationship between weight loss observed over the used catalysts and temperatures. The order of carbon deposition is $Ni/La_2O_3 > 9\%$

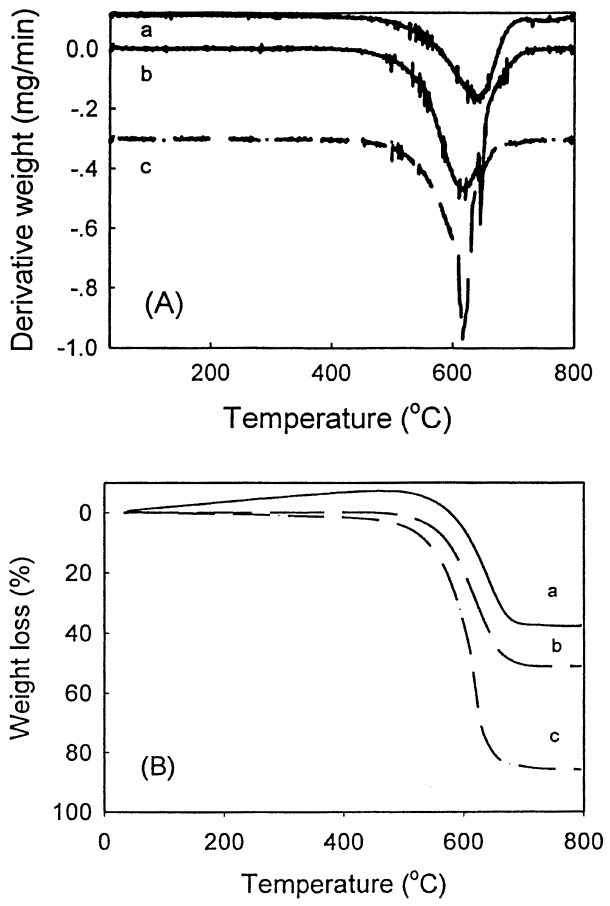

Figure 8. (A) DTG and (B) TG profiles observed over used catalyst: (a) La_2NiO_4 (sol–gel) (80 h); (b) 9% $La_2NiO_4/\gamma Al_2O_3$ (30 h); (c) Ni/La_2O_3 (4 h); the data in parentheses are on-stream time.

La_2NiO_4/γ-$Al_2O_3 > La_2NiO_4$ (sol–gel). In addition, one can see that for a used La_2NiO_4 (sol–gel) catalyst, there was a gain in weight below 550 °C (figure 8(B, a)) due to oxygen adsorption. The existence of non-stoichiometric oxygen in La_2NiO_4 (sol–gel) has been confirmed by the results of O_2 TPD studies (figure 3). We suggested that non-stoichiometric oxygen in La_2NiO_4 (sol–gel) has a role to play in the CO_2 reforming of CH_4.

4. Conclusion

A La_2NiO_4 catalyst was generated according to a sol–gel method, and its catalytic performance was evaluated for the CH_4/CO_2 reforming reaction. The results show that CH_4 and CO_2 conversions and CO and H_2 selectivities over this catalyst are significantly higher than those observed over Ni/La_2O_3 and 9% La_2NiO_4/γ-Al_2O_3, and carbon deposition is the least over the sol–gel-generated La_2NiO_4 catalyst. The XRD results confirm that La_2NiO_4 (sol–gel) exhibited a typical spinel structure. During CH_4/CO_2 reforming, the active Ni^0 particles did not aggregate and sinter, and the catalyst showed good stability within an on-stream time of 80 h.

Acknowledgment

This work was supported by the Research Grants Council of the Hong Kong Special Administration Region, China (Project No. HKBU 2053/98P).

References

[1] A.M. Gadalla and B. Bower, Chem. Eng. Sci. 43 (1988) 3049.
[2] J.H. Edwards, K.T. Do, A.H. Maitra, S. Schuck and W. Stein, Sol. Eng. 1 (1995) 389.
[3] J.D. Fish and D.C. Hawn, J. Sol. Energy Eng. 109 (1987) 215.
[4] B. Delmon, Appl. Catal. B: Environ. 1 (1992) 139.
[5] N.R. Udengaard, J.H.B. Hansen and D.C. Hanson, Oil Gas J. 90 (1992) 62.
[6] Z. Zhang and X.E. Verkyios, J. Chem. Soc. Chem. Commun. (1995) 71.
[7] Z. Zhang and X.E. Verkyios, Catal. Today 21 (1994) 589.
[8] Y.H. Hu and E. Ruckenstein, Catal. Lett. 57 (1999) 167; 36 (1996) 145.
[9] E. Ruckenstein and Y.H. Hu, Appl. Catal. A: Gen. 133 (1995) 149.
[10] Z. Zhang, X.E. Verkyios, S.M. MacDonald and S. Affrossman, J. Phys. Chem. 100 (1996) 744.
[11] Z. Zhang and X.E. Verkyios, Appl. Catal. A: Gen. 138 (1996) 109.
[12] Z. Cheng. Q. Wu, J. Li and Q. Zhu, Catal. Today 30 (1996) 147.
[13] T. Horiuchi, K. Sakuma, F. Takehisa, Y. Kubo, T. Osaki and T. Mori, Appl. Catal. A: Gen. 144 (1996) 111.
[14] E. Ruckenstein and Y.H. Hu, J. Catal. 162 (1996) 230.
[15] Y. Chen and J. Ren, Catal. Lett. 29 (1994) 39.
[16] V.R. Choudhary and A.M. Rajput, Ind. Eng. Chem. Res. 25 (1996) 3934.
[17] J.R. Rostrup-Nielsen and J.H. Bak-Hansen, J. Catal. 144 (1993) 38.
[18] O. Yamazki, T. Nozaki, K. Omata and K. Fujimoto, Chem. Lett. (1992) 1953.
[19] J.M. Rynkowski, T. Paryjczak and M. Lenik, Appl. Catal. A: Gen. 126 (1995) 257.
[20 J.A. Pena, C. Herguido, C. Guimon, A. Monzon and J. Santamaria, J. Catal. 159 (1996) 313.
[21] M.A. Pena and J.L. Fierrio, Chem. Rev. 101 (2001) 1997.
[22] Y.J. Ren, W.S. Yang, S.S. Sheng, G.X. Xiong and L.W. Lin, Chinese J. Catal. 19 (1998) 541.
[23] B.S. Liu, L.Z. Gao and C.T. Au, Appl. Catal. A: Gen. 235 (2002) 193.
[24] S. Ho and T. Chou, Ind. Eng. Chem. Res. 34 (1995) 2279.
[25] Q. Liang, L.Z. Gao, Q. Li, S.H. Tang, B.C. Liu and Z.L. Yu, Carbon 39 (2001) 897.
[26] J.Z. Luo, Z.L. Yu, C.F. Ng and C.T. Au, J. Catal. 194 (2000) 198.
[27] B.S. Liu, Y. Yang and A. Sayari, Appl. Catal. A: Gen. 214 (2001) 95.